

AD-E400 118

AD

14

TECHNICAL REPORT ARLCB-TR-77038

12

AD A 052670

DDC FILE COPY

VIBRATIONS OF A HELICOPTER ROTOR BLADE USING FINITE ELEMENT-UNCONSTRAINED VARIATIONAL FORMULATIONS

J. J. Wu  
C. N. Shen

September 1977



US ARMY ARMAMENT RESEARCH AND DEVELOPMENT COMMAND  
LARGE CALIBER WEAPON SYSTEM LABORATORY  
BENÉT WEAPONS LABORATORY  
WATERVLIET, N. Y. 12189

AMCMS No. 611102.11.H4500  
DA Project No. 1L161102AH45  
PRON No. EJ-7-Y0011-01-EJ-M7

DDC  
RECEIVED  
APR 13 1978  
B

DISTRIBUTION STATEMENT A  
Approved for public release;  
Distribution Unlimited

410 220 JOB

#### DISCLAIMER

The findings in this report are not to be construed as an official Department of the Army position unless so designated by other authorized documents.

The use of trade name(s) and/or manufacturer(s) does not constitute an official indorsement or approval.

#### DISPOSITION

Destroy this report when it is no longer needed. Do not return it to the originator.



SECURITY CLASSIFICATION OF THIS PAGE (When Data Entered)

REPORT DOCUMENTATION PAGE		READ INSTRUCTIONS BEFORE COMPLETING FORM
1. REPORT NUMBER <b>24</b> ARLCB-TR-77038	2. GOVT ACCESSION NO.	3. RECIPIENT'S CATALOG NUMBER
4. TITLE (and Subtitle) <b>6</b> VIBRATIONS OF A HELICOPTER ROTOR BLADE USING FINITE ELEMENT-UNCONSTRAINED VARIATIONAL FORMULATIONS.	5. TYPE OF REPORT & PERIOD COVERED <b>9</b> Technical rept.	
7. AUTHOR(s) <b>20</b> J.J. Wu C.N. Shen	8. CONTRACT OR GRANT NUMBER(s)	
9. PERFORMING ORGANIZATION NAME AND ADDRESS Benet Weapons Laboratory Watervliet Arsenal, Watervliet, N.Y. 12189 DRDAR-LCB-TL	10. PROGRAM ELEMENT, PROJECT, TASK AREA & WORK UNIT NUMBERS AMCMS No. 61102 11 H4500 DA Proj. No. 11161102AH45 PRON No. EJ-7-Y0011-01-EJ-M7	
11. CONTROLLING OFFICE NAME AND ADDRESS US Army Armament Research and Development Command Large Caliber Weapon System Laboratory Dover, New Jersey 07801	12. REPORT DATE <b>11</b> September 1977	
14. MONITORING AGENCY NAME & ADDRESS (if different from Controlling Office) <b>18</b> SBIE <b>19</b> AD-E400118	13. NUMBER OF PAGES <b>32</b> 31p 30	
15. SECURITY CLASS. (of this report) UNCLASSIFIED		15a. DECLASSIFICATION/DOWNGRADING SCHEDULE
16. DISTRIBUTION STATEMENT (of this Report) Approved for public release; distribution unlimited.		
17. DISTRIBUTION STATEMENT (of the abstract entered in Block 20, if different from Report)		
18. SUPPLEMENTARY NOTES		
19. KEY WORDS (Continue on reverse side if necessary and identify by block number) Beams (Radiation)      Rotation Coupling Effect      Stability Dynamics              Vibration Flutter Helicopter Rotors		
20. ABSTRACT (Continue on reverse side if necessary and identify by block number) In the past several years, a numerical method has been developed which is a generalized Rayleigh-Ritz - finite element discretization using the combined concept of Lagrange multipliers and adjoint variables. This approach enables one to deal with problems associated with nonconservative forces, coupling effects and all types of boundary conditions in a routine fashion; and it appears promising in solving the vibration and dynamic stability problems associated with the complicated equations of a helicopter rotor blade. This paper presents (Continued on reverse side)		

over

Block 20 (cont)

the first application of the general method of the vibration problem of such a rotor blade.

The basic differential equations in this paper are taken from the linear, but fully coupled set developed by Houbolt and Brooks in 1956. These equations are further reduced to a simplest possible case and yet still contain the coupling of flap and root torsion modes. An unconstrained, adjoint variational statement has been established which is both the necessary and sufficient condition for the coupled differential equations and some general, but physical meaningful boundary conditions. The finite element matrix equations are then derived from this variational statement illustrating the way that coupling terms could be handled in general.

The numerical results from some demonstrative examples show that instability of flutter can occur in the range of operational rotor speed due to the coupled motion of flapping and root torsion without any aerodynamic force, if the torsional spring (or the pitch control link) is not sufficiently stiff. This instability does not appear to have been reported previously.

ACCESSION for	
NTIS	White Section <input checked="" type="checkbox"/>
DDC	Buff Section <input type="checkbox"/>
UNANNOUNCED	<input type="checkbox"/>
JUSTIFICATION _____	
BY _____	
DISTRIBUTION/AVAILABILITY CODES	
Dist.	AVAIL. and/or SPECIAL
A	



## TABLE OF CONTENTS

	Page
1. Introduction	1
2. Statement of the Problem - Differential Equations	2
3. An Unconstrained Variational Statement and Boundary Conditions	5
4. Matrix Equations From Finite Element Discretization	8
5. Results and Discussion	13
Acknowledgement	14
References	15
Appendix	16

## LIST OF ILLUSTRATIONS

### Figure

1. Problem Configuration.	19
2. Parameters Related to Off-sets of Various Axes.	20
3. Vibration Frequency vs Speed of Rotation ( $e_A = 0.0030$ , $e = 0.0030$ ) - No Instability in the Range of Speed Shown.	21
4. Vibration Frequency vs Speed of Rotation ( $e_A = 0.0015$ , $e = 0.0030$ ) - No Instability in the Range of Speed Shown.	22
5. Vibration Frequency vs Speed of Rotation ( $e_A = 0$ , $e = 0.0030$ ) - Flutter Instability at $\Omega=16.46$ .	23
6. Vibration Frequency vs Speed of Rotation ( $e_A = -0.0015$ , $e = 0.0030$ ) - Flutter Instability at $\Omega=5.80$ .	24
7. Vibration Frequency vs Speed of Rotation ( $e_A = -0.0030$ , $e = 0.0030$ ) - Flutter Instability at $\Omega=4.59$ .	25
8. Vibration Frequency vs Speed of Rotation. (Same data as in Figure 5 except $k_3$ has been changed from zero to 0.01) - Flutter Instability at $\Omega=17.08$ .	26

1. INTRODUCTION. An analytical investigation on vibrations and dynamic stability of helicopter rotor blades usually consists of two phases (1) the derivation of the governing differential equations to include parameters and variables considered physically important, and (2) the formulation of solutions for the equations derived and data interpretations. This paper deals with the second phase of such an investigation.

Due to the slenderness of a helicopter rotor blades, its aerodynamic cross-section and the requirements on the craft's maneuverability, there are a large number of interacting parameters and the resulting differential equations are, as a rule, nonlinear, coupled in terms of field variables. In addition, the aerodynamic forces, coriolis forces due to rotation of the blade are nonconservative in nature and the effects due to structural damping and various boundary conditions must be evaluated.

Considerable attention has been given recently to the derivation of a consistent set of nonlinear differential equations together with aerodynamic forces. This fact is amply demonstrated by the work of Friedman and Tong [1] and that of Hodges and Ormiston [2]. In both references [1] and [2], brief reviews on earlier work on helicopter blade equations can be found. As for obtaining solutions to these equations, there does not appear to exist a general and efficient method to deal with the difficulties associated with nonlinearities, nonconservative forces, coupling terms, various boundary conditions, damping effects and periodic excitations. For example, Miller and Ellis [3], Ham [4], and Friedman and Tong [1] have obtained approximate solution by including in their solution formulation only the lowest modes of vibrations, Hodges and Ormiston [2,5] employed the Galerkin technique in their numerical examples. One of the disadvantages of this approach is its inability to handle general boundary conditions.

Using the combined concept of adjoint variable and Lagrange multipliers, variational statements can be established for a wide range of linear problems with nonconservative forces and very versatile boundary conditions [6]. Thus a generalized Rayleigh-Ritz approximation scheme can be established for the obtaining of solutions of these otherwise difficult-to-solve problems. In conjunction with finite element discretization, this approach has been amply demonstrated in such applications as nonconservative stability, damping effects and very general boundary conditions [7,8,9]. In the present study, the solution formulation is limited to the blade vibration considering only the coupling of flapping and root torsion. Although the present method can conceivably be extended for solutions of nonlinear problems, it is desirable first to have a thorough understanding to solutions of linear problems. For this purpose, one can go back two decades and use the equations consistently derived by Houbolt and Brooks in 1956 [10]. The original set of equations was derived for elastic distributed torsion. It can be adapted to model root torsion if proper boundary conditions are introduced. This is shown in Sections 1 and 2. The physical justification for emphasizing root torsion over the distributed torsion was due to the pitch control link at the inboard end of the blade and was used by Miller and Ellis [3] and again by Ham [4]. It should be clear that, in the present formulation, to include distributed torsion is simply a matter of increasing the number of degrees-of-freedom of the discrete system. The basis of the solution formulation and the technique of handling the coupling



terms are given in Sections 2 and 3. Finally, the numerical results obtained indicate that "flutter instability" can occur simply due to the coupling effect considered without any aerodynamic loads.

2. STATEMENT OF THE PROBLEM - DIFFERENTIAL EQUATIONS. As a first step to demonstrate the application of the unconstrained variational - finite element formulation to helicopter rotors, the vibration of a rotor blade considering the coupling of flap and root torsion modes of motion is analyzed (Figure 1). For this purpose, the linear set of equations, derived by Houbolt and Brooks [10], including the coupling flap and distributed torsion is rewritten here:

$$(EIw'' - Te_A\phi)'' - (Tw')' - (\Omega^2 m x e \phi)' + m(\ddot{w} + e\ddot{\phi}) = L_z, \quad (1)$$

$$- [(GJ + Tk_A^2)\phi']' - Te_A w'' + \Omega^2 m x e w' + \Omega^2 m (k_{m2}^2 - k_{m1}^2 + e e_0)\phi + m k_m^2 \ddot{\phi} + m e \ddot{w} = M \quad (2)$$

where  $w = w(x,t)$  and  $\phi = \phi(x,t)$  denote the flapping deflection and distributed torsion of the rotor blade respectively. A prime (') denotes differentiation with respect to  $x$ , the coordinate along the blade elastic axis and a dot (·), differentiation with respect to the time  $t$ . Other symbols are defined in the following and are consistent with the notation in reference [10].

- $EI$  = flexural rigidity of the cross section.
- $GJ$  = torsional rigidity of the cross section.
- $l$  = length of the blade.
- $e$  = chordwise distance between elastic axis (E.A.) and centre of gravity (C.G.) of a cross-section, positive if C.G. is ahead of E.A.
- $e_A$  = chordwise distance between E.A. and centre of tensile area (C.T.) of a cross section, positive if C.T. is ahead of E.A.
- $e_0$  = chordwise distance at the root between E.A. and the axis about which the blade is rotating, positive if E.A. is ahead.
- $k_A$  = polar radius of a gyration of the tensile area of a cross-section w.r.t. E.A. in a cross-section.
- $k_{m1}$  = radius of gyration of the total area of a cross-section about the major neutral axis (axis 1-1 in Figure 2).
- $k_{m2}$  = radius of gyration of the total area of a cross-section about an axis perpendicular to the major neutral axis and through E.A. (axis m2-m2 in Figure 2).

$k_m$  = polar radius of gyration of the total area of cross-section about E.A. ( $k_m^2 = k_{m1}^2 + k_{m2}^2$ ).

$\Omega$  = blade angular velocity.

$T = T(x) = \int_x^l m\Omega^2 x dx$ , which is the tensile force at location  $x$ .

$L_z$  = aerodynamic lift per unit length of the blade.

$M$  = aerodynamic torque per unit length of the blade.

In reference [10], a more general set of linear equations with fully coupled flap, lag and distributed torsion modes of motion were derived. The coupling terms have been shown to be due to the noncoincidence of the elastic centre, centre of gravity and tension centre, the centrifugal force and the built-in angle of twist. For a rotor blade without the built-in twist angle, the lag mode of motion is uncoupled from the general set of equations and the remaining coupled equations are Eqs. (1) and (2) considered here.

Since only the "free vibration" of the rotor blade with a coupling between flexural and root torsion is considered in this paper, the terms due to aerodynamic forces are set to zero and the torsional displacement is only a function of time and not a function of  $x$ . Thus

$$M = L_z = 0, \quad \phi = \phi(t) \quad (3)$$

and Eqs. (1) and (2) reduce to the following:

$$EIw'''' - (Tw')' + m\ddot{w} - \Omega^2 m e \phi + m e \ddot{\phi} = 0 \quad (4)$$

$$\begin{aligned} \Omega^2 m (k_{m2}^2 - k_{m1}^2 + e e_0) \phi + m k_m^2 \ddot{\phi} - T e_A w'' \\ + m \Omega^2 e x w' + m e \ddot{w} = 0 \end{aligned} \quad (5)$$

In Eqs. (4) and (5), it is also assumed that the blade has constant  $E$ ,  $I$  and  $m$  throughout its length. To simplify solution formulations as much as possible, Eqs. (4) and (5) will be transformed into dimensionless forms and appropriate dimensionless parameters will be introduced. This process will also facilitate parametric studies.

Let

$$\bar{w} = \frac{w}{l}, \quad \bar{\phi} = \phi$$

$$\bar{x} = \frac{x}{l}, \quad \bar{t} = \frac{t}{c} \quad (6)$$

where the constant  $c$  has a real time dimension and will be defined later in Eqs. (12). Eqs. (4) and (5) become



$$\frac{EI\ell}{\ell^4} \frac{\partial^2 \bar{w}}{\partial \bar{x}^4} - \frac{\ell}{\ell^4} \frac{\partial}{\partial \bar{x}} \left( T \frac{\partial \bar{w}}{\partial \bar{x}} \right) + \frac{m\ell}{c^2} \frac{\partial^2 \bar{w}}{\partial \bar{t}^2} - m\Omega^2 e \bar{\phi} + \frac{me}{c^2} \frac{\partial^2 \bar{\phi}}{\partial \bar{t}^2} = 0 \quad (7)$$

and

$$m\Omega^2 k^2 \bar{\phi} + \frac{mk_m^2}{c^2} \frac{\partial^2 \bar{\phi}}{\partial \bar{t}^2} - \frac{T e_A \ell}{\ell^2} \frac{\partial^2 \bar{w}}{\partial \bar{x}^2} + \frac{m\Omega^2 e \ell^2}{\ell} \bar{x} \frac{\partial \bar{w}}{\partial \bar{x}} + \frac{me\ell}{c^2} \frac{\partial^2 \bar{w}}{\partial \bar{t}^2} = 0 \quad (8)$$

where

$$k^2 = k_{m2}^2 - k_{m1}^2 + ee_0 \quad (9)$$

Multiplying Eq. (7) by  $\frac{\ell^3}{EI}$ , one has

$$\begin{aligned} \frac{\partial^4 \bar{w}}{\partial \bar{x}^4} - \frac{\partial}{\partial \bar{x}} \left( \frac{T\ell^2}{EI} \frac{\partial \bar{w}}{\partial \bar{x}} \right) + \frac{m\ell^4}{EI} \frac{1}{c^2} \frac{\partial^2 \bar{w}}{\partial \bar{t}^2} - \frac{m\ell^4}{EI} \frac{e}{\ell} \frac{1}{c^2} c^2 \Omega^2 \bar{\phi} \\ + \frac{m\ell^4}{EI} \frac{1}{c^2} \frac{e}{\ell} \frac{\partial^2 \bar{\phi}}{\partial \bar{t}^2} = 0 \end{aligned} \quad (10)$$

Multiplying Eq. (8) by  $\frac{c^2}{m\ell^2}$ , one has

$$c^2 \Omega^2 \frac{k^2}{\ell^2} \bar{\phi} + \frac{k_m^2}{\ell^2} \frac{\partial^2 \bar{\phi}}{\partial \bar{t}^2} - \frac{c^2 T}{m\ell^2} \frac{e_A}{\ell} \frac{\partial^2 \bar{w}}{\partial \bar{x}^2} + c^2 \Omega^2 \frac{e}{\ell} \bar{x} \frac{\partial \bar{w}}{\partial \bar{x}} + \frac{e}{\ell} \frac{\partial^2 \bar{w}}{\partial \bar{t}^2} = 0 \quad (11)$$

Now let

$$\left. \begin{aligned} c^2 &= \frac{m\ell^2}{EI} \\ \bar{e} &= \frac{e}{\ell}, \quad \bar{e}_A = \frac{e_A}{\ell}, \quad \bar{e}_0 = \frac{e_0}{\ell} \\ \bar{k} &= \frac{k}{\ell}, \quad \bar{k}_m = \frac{k_m}{\ell} \\ \bar{\Omega} &= c\Omega \\ \bar{T}(\bar{x}) &= \frac{T(x)\ell^2}{EI} = \frac{1}{2} \bar{\Omega}^2 (1 - \bar{x}^2) \end{aligned} \right\} \quad (12)$$

Eqs. (10) and (11) then become

$$\frac{\partial^4 \bar{w}}{\partial \bar{x}^4} - \frac{\partial}{\partial \bar{x}} \left( \bar{T}(\bar{x}) \frac{\partial \bar{w}}{\partial \bar{x}} \right) + \frac{\partial^2 \bar{w}}{\partial \bar{t}^2} - \bar{\Omega}^2 \bar{e} \bar{\phi} + \bar{e} \frac{\partial^2 \bar{\phi}}{\partial \bar{t}^2} = 0 \quad (13)$$

and

$$\bar{\Omega}^2 \bar{k}^2 \bar{\phi} + k_m^2 \frac{\partial^2 \bar{\phi}}{\partial \bar{t}^2} - \bar{T}(\bar{x}) \bar{e}_A \frac{\partial^2 \bar{w}}{\partial \bar{x}^2} + \bar{\Omega}^2 \bar{e} \bar{x} \frac{\partial \bar{w}}{\partial \bar{x}} + \bar{e} \frac{\partial^2 \bar{w}}{\partial \bar{t}^2} = 0 \quad (14)$$

With all quantities in Eqs. (13) and (14) in dimensionless forms, one can omit the bars altogether and write:

$$w'''' - (Tw')' + \ddot{w} - \Omega^2 e \phi + e \ddot{\phi} = 0 \quad (15)$$

and

$$\Omega^2 k^2 \phi + k_m^2 \ddot{\phi} - T e_A w''' + \Omega^2 e x w' + e \ddot{w} = 0 \quad (16)$$

Furthermore, it is assumed that

$$w(x, t) = w(x) e^{\lambda t} \quad (17)$$

$$\phi(t) = \phi e^{\lambda t}$$

Thus the final set of equations upon which the present solution formulations are based, is the following:

$$w'''' - (Tw')' + \lambda^2 w - \Omega^2 e \phi + \lambda^2 e \phi = 0 \quad (18)$$

and

$$\Omega^2 k^2 \phi + \lambda^2 k_m^2 \phi - T e_A w''' + \Omega^2 e x w' + \lambda^2 e w = 0 \quad (19)$$

### 3. AN UNCONSTRAINED VARIATIONAL STATEMENT AND BOUNDARY CONDITIONS.

Some of the unique features of the unconventional variational formulation are that all the boundary conditions are natural boundary conditions and that the set of the differential equations, together with all the boundary conditions, is the direct consequence of a variational statement and vice versa. The construction of such a variational statement is simply a process of integration-by-parts from a bilinear functional of the original differential equations multiplied by the variation of the adjoint field variable, into some other bilinear functional with lowest possible derivations of both the original field variable and the variations of the adjoint variable. With a proper choice of the generalized Lagrange multipliers, any physical meaningful boundary conditions consistent with the physical meaning of the given differential equations themselves can be resulted from the variational statement as natural boundary conditions. This general process was treated elsewhere [7] and will not be reported here. Presently, an unconstrained variational statement will be given which leads to the original differential equations and a set of a very general boundary conditions.



Let us consider the variational statement

$$\delta I = 0 \quad (20a)$$

with

$$I = I_1 + I_2 \quad (20b)$$

$$I_1 = \int_0^1 [w'w^{*''} + Tw'w^{*'} + \lambda^2 ww^* + e(\lambda^2 - \Omega^2)\phi w^*] dx \\ + k_1 w(0)w^*(0) + k_2 w'(0)w^{*'}(0) \quad (20c)$$

and

$$I_2 = \int_0^1 [\Omega^2 k^2 + \lambda^2 k_m^2] \phi \phi^* + e_A T' w' \phi^* + e(\Omega^2 x w' \phi^* + \lambda^2 w \phi^*) dx + k_3 \phi \phi^* \quad (20d)$$

where a star(\*) denotes the adjoint variables and the variations are totally unconstrained. The Lagrange multipliers  $k_1$ ,  $k_2$  and  $k_3$  are the spring constants, in dimensionless form, for deflection, bending and torsion at the hub ( $x = 0$ ) respectively. To show that the unconstrained variational statement of Eqs. (20) leads to the original differential equations and the necessary boundary conditions, one considers

$$(\delta I)_{w,\phi} = 0 \quad (21a)$$

where  $(\delta I)_{w,\phi}$  means taking the variation of  $I$  with  $w, \phi$  not varied. Thus

$$(\delta I)_{w,\phi} = (\delta I_1)_{w,\phi} + (\delta I_2)_{w,\phi} = 0 \quad (21b)$$

with

$$(\delta I_1)_{w,\phi} = \int_0^1 [w' \delta w^{*''} + Tw' \delta w^{*'} + \lambda^2 w \delta w^* + e(\lambda^2 - \Omega^2) \phi \delta w^*] dx \\ + k_1 w(0) \delta w^*(0) + k_2 w'(0) \delta w^{*'}(0) \quad (21c)$$

and

$$(\delta I_2)_{w,\phi} = \int_0^1 [(\Omega^2 k^2 + \lambda^2 k_m^2) \phi \delta \phi^* + e_A T' w' \delta \phi^* \\ + e(\Omega^2 x w' + \lambda^2 w) \delta \phi^*] dx + k_3 \phi \delta \phi^* \quad (21d)$$

Performing integration-by-parts, one arrives at

$$\begin{aligned}
 (\delta I_1)_{w,\phi} &= \int_0^1 [w'''' - (Tw')' + \lambda^2 w + e(\lambda^2 - \Omega^2)\phi] \delta w^* dx \\
 &+ w''(1) \delta w^*(1) - [w''(1) - T(1)w'(1)] \delta w^*(1) \\
 &- [w''(0) - k_2 w'(0)] \delta w^*(0) \\
 &+ [w'''(0) - T(0)w'(0) + k_1 w(0)] \delta w^*(0)
 \end{aligned} \tag{22a}$$

and

$$\begin{aligned}
 (\delta I_2)_{w,\phi} &= \int_0^1 [(\Omega^2 k^2 + \lambda^2 k_m^2)\phi - e_A T w'' + e(\Omega^2 x w' + \lambda^2 w)] \delta \phi^* dx \\
 &+ [e_A T(1)w'(1) - e_A T(0)w'(0) + k_3 \phi] \delta \phi^*
 \end{aligned} \tag{22b}$$

Thus Eqs. (21) is the necessary and sufficient condition for the following differential equations and boundary conditions:

D.E.:

$$w'''' - (Tw')' + \lambda^2 w + e(\lambda^2 - \Omega^2)\phi = 0 \tag{23a}$$

$$(\Omega^2 k^2 + \lambda^2 k_m^2)\phi - e_A T w'' + e(\Omega^2 x w' + \lambda^2 w) = 0 \tag{23b}$$

B.C.:

$$w''(1) = 0, \quad w'''(1) = 0 \tag{24a, 24b}$$

$$w''(0) - k_2 w'(0) = 0 \tag{24c}$$

$$w'''(0) - \frac{\Omega^2}{2} w'(0) + k_1 w(0) = 0 \tag{24d}$$

and

$$-\frac{e_A}{2} \Omega^2 w'(0) + k_3 \phi = 0 \tag{24e}$$

Note that in Eqs. (24) the fact that

$$T(1) = 0$$

and

$$T(0) = \frac{1}{2} \Omega^2 \tag{25}$$

has been used.



It is observed that the boundary conditions of Eqs. (24c) and (24d) represent very general support conditions at the hub. The special case  $k_1 = \infty$  and  $k_2 = 0$  corresponds to a hinged blade, while the case  $k_1 = \infty$ ,  $k_2 = \infty$  corresponds to a hingeless blade. These two special cases are the only ones considered in the literature. The boundary condition (24e) indicates a coupling between the flexural motion  $w$  and root torsion at the hub due to the centrifugal forces and the noncoincidence of the elastic axis and the tension axis.

4. MATRIX EQUATIONS FROM FINITE ELEMENT DISCRETIZATION. In this section, we shall briefly describe the formulation of the matrix equation of the approximate solution from the variational statement given in the previous section. From Eqs. (21), one can write

$$(\delta I)_{w,\phi} = 0;$$

or,

$$\begin{aligned} (\delta I)_{w,\phi} = & \int_0^1 (w' \delta w^{*''} + T w' \delta w^{*'} - e \Omega^2 \phi \delta w^*) dx \\ & + k_1 w(0) \delta w^*(0) + k_2 w'(0) \delta w^{*'}(0) + \lambda^2 \int_0^1 (w \delta w^* + e \phi \delta w^*) dx \\ & + \int_0^1 [\Omega^2 k^2 \phi \delta \phi^* + e_A T' w' \delta \phi^* + e \Omega^2 x w' \delta \phi^*] dx + k_3 \phi \delta \phi^* \\ & + \lambda^2 \int_0^1 (k_m^2 \phi \delta \phi^* + e w \delta \phi^*) dx \end{aligned} \quad (26)$$

It should be noted that Eq. (26) is a quite general equation. Various types of approximate solutions can be obtained depending on the choice of the coordinate functions. The motivation of using the finite element discretizations, which corresponds to the choice of a set of piecewise analytic functions, is twofold: for the ease of extending this formulation to problems of irregular geometry and for the adaptations to general finite element computer systems.

In the present formulation, however, only blades of uniform cross-sections will be considered and the elements are assumed to be of the same length. Thus, one introduces a local (element) coordinate  $\xi$  which relates to the global (entire blade) coordinate  $x$  such that

$$\xi = \xi^{(i)} = L(x - \frac{i-1}{L}) \quad (27)$$

where  $L$  is the number of elements and  $i$  denotes the  $i$ -th element. Using the notation

$$w^{(i)}(\xi) = w[x(\xi^{(i)})], \text{ etc.} \quad (28)$$

for simplicity and noting that

$$d\xi = L dx$$

$$w'(x) = L w^{(i)'(\xi)}, \text{ etc.} \quad (29)$$

one then has, from Eq. (26):

$$\begin{aligned}
 (\delta I)_{w, \phi} &= 0 \\
 &= \sum_{i=1}^L \left\{ \int_0^1 L^3 w^{(i)}(\xi) \delta w^{*(i)}(\xi) d\xi \right. \\
 &+ \int_0^1 L T^{(i)}(\xi) w^{(i)}(\xi) \delta w^{*(i)}(\xi) d\xi - \frac{e\Omega^2 \phi}{L} \int_0^1 \delta w^{*(i)}(\xi) d\xi \left. \right\} \\
 &+ k_1 w^{(1)}(0) \delta w^{*(1)}(0) + k_2 L^2 w^{(i)}(0) \delta w^{*(i)}(0) \\
 &+ \lambda^2 \sum_{i=1}^L \left\{ \frac{1}{L} \int_0^1 w^{(i)}(\xi) \delta w^{*(i)}(\xi) d\xi + \frac{e\phi}{L} \int_0^1 \delta w^{*(i)}(\xi) d\xi \right\} \\
 &- \sum_{i=1}^L \left\{ \Omega^2 k^2 \phi \delta \phi^* \frac{1}{L} \int_0^1 d\xi^{(i)} + e_A L \int_0^1 T^{(i)}(\xi) w^{(i)}(\xi) d\xi \delta \phi^* \right. \\
 &+ \frac{e\Omega^2}{L} \int_0^1 [\xi + (i-1)] w^{(i)}(\xi) d\xi \delta \phi^* \left. \right\} + k_3 \phi \delta \phi^* \\
 &+ \lambda^2 \left\{ \frac{k_m^2}{L} \phi \delta \phi^* \int_0^1 d\xi^{(i)} + \sum_{i=1}^L \frac{e}{L} \int_0^1 w^{(i)}(\xi) d\xi \right\} \delta \phi^* \tag{30}
 \end{aligned}$$

where

$$T^{(i)}(\xi) = -b[\xi^2 + 2(i-1)\xi + (i-1)^2 - L^2] \tag{31}$$

and

$$b = \frac{\Omega^2}{2L^2} \tag{32}$$

At this point, it is appropriate to introduce the shape function and generalized coordinates. Let

$$\begin{aligned}
 w^{(i)}(\xi) &= \underline{a}^T(\xi) \underline{w}^{(i)} \\
 w^{*(i)}(\xi) &= \underline{a}^T(\xi) \underline{w}^{*(i)} \tag{33}
 \end{aligned}$$

where the superscript T denotes the transpose of a matrix,



$$\begin{aligned}\tilde{w}^{(i)T} &= \{ w_1^{(i)} \quad w_2^{(i)} \quad w_3^{(i)} \quad w_4^{(i)} \} \\ \tilde{w}^{*(i)T} &= \{ w_1^{*(i)} \quad w_2^{*(i)} \quad w_3^{*(i)} \quad w_4^{*(i)} \}\end{aligned}\quad (34)$$

and

$$\underline{a}^T(\xi) = \{1 - 3\xi^2 + 2\xi^3, \quad \xi - 2\xi^2 + \xi^3, \quad 3\xi^2 - 2\xi^3, \quad -\xi^2 + \xi^3\} \quad (35)$$

Using Eqs. (31), (32) and in terms of  $w^{(i)}$ ,  $w^{*(i)}$ , Eq. (30) becomes

$$\begin{aligned}(\delta I)_{w,\phi} &= 0 \\ &= \sum_{i=1}^L \delta w^{*(i)T} \{ L^3 \int_0^1 a' a''^T d\xi - bL [\int_0^1 \xi^2 a' a'^T d\xi + 2(i-1) \int_0^1 \xi a' a'^T d\xi \\ &\quad + \{L^2 - (i-1)^2\} \int_0^1 a' a'^T d\xi] \tilde{w}^{(i)} \} \\ &\quad + \sum_{i=1}^L \delta w^{*(1)T} (-2ebL) \int_0^1 a d\xi \phi \\ &+ \delta w^{*(1)T} k_1 \underline{a}(0) \underline{a}^T(0) \tilde{w}^{(1)} + \delta w^{*(1)} k_2 L^2 \underline{a}'(0) \underline{a}'^T(0) \tilde{w}^{(1)} \\ &\quad + \lambda^2 \{ \sum_{i=1}^L \delta w^{*(i)T} \frac{1}{L} \int_0^1 a a^T d\xi \tilde{w}^{(i)} + \frac{e}{L} \int_0^1 a d\xi \phi \} \\ &\quad + \delta \phi^* \Omega^2 k^2 \phi + \delta \phi^* k_3 \phi \\ &+ \delta \phi^* \sum_{i=1}^L 2(e - e_A) bL \int_0^1 \xi a'^T(\xi) d\xi + (i-1) \int_0^1 a'^T d\xi \tilde{w}^{(i)} \\ &\quad + \lambda^2 \delta \phi^* [k_m^2 \phi + \sum_{i=1}^L \frac{e}{L} \int_0^1 a^T d\xi \tilde{w}^{(i)}] \end{aligned}\quad (36)$$

Or,

$$\begin{aligned}
 & (\delta I)_{w, \phi} = 0 \\
 & = \sum_{i=1}^L \delta \underline{w}^{*(i)T} \{L^3 \underline{C} - bL[\underline{E} + 2(i-1)\underline{D}] - (L^2 - (i-1)^2) \underline{B}\} \underline{w}^{(i)} \\
 & \quad + \sum_{i=1}^L \delta \underline{w}^{*(i)T} (-2ebL) \underline{p} \phi + \delta \underline{w}^{*(i)T} [k_1 \underline{F} + k_2 L \underline{G}] \underline{w}^{(1)} \\
 & \quad + \lambda^2 \left[ \sum_{i=1}^L \delta \underline{w}^{*(i)T} \left[ \frac{1}{L} \underline{A} \underline{w}^{(i)} + \frac{e}{L} \underline{p} \phi \right] \right. \\
 & \quad \left. + \delta \phi^* \sum_{i=1}^L 2(e - e_A) bL (\underline{s}^T + (i-1) \underline{r}^T) \underline{w}^{(i)} \right. \\
 & \quad \left. + \delta \phi^* (\Omega^2 k^2 + k_3) \phi + \lambda^2 \delta \phi^* \left( \sum_{i=1}^L \frac{e}{L} \underline{p}^T \underline{w}^{(i)} + k_m^2 \phi \right) \right. \quad (37)
 \end{aligned}$$

where the element matrices are defined as follows,

$$\begin{aligned}
 \underline{A} &= \int_0^1 \underline{a} \underline{a}^T d\xi, & \underline{B} &= \int_0^1 \underline{a}' \underline{a}'^T d\xi, & \underline{C} &= \int_0^1 \underline{a}'' \underline{a}''^T d\xi \\
 \underline{D} &= \int_0^1 \xi \underline{a}' \underline{a}'^T d\xi, & \underline{E} &= \int_0^1 \xi^2 \underline{a}' \underline{a}'^T d\xi \\
 \underline{F} &= \underline{a}(0) \underline{a}^T(0), & \underline{G} &= \underline{a}'(0) \underline{a}'^T(0) \\
 \underline{p} &= \int_0^1 \underline{a} d\xi, & \underline{r} &= \int_0^1 \underline{a}' d\xi, & \underline{s} &= \int_0^1 \xi \underline{a}' d\xi \quad (38)
 \end{aligned}$$

The numerical values of these matrices are given in the Appendix.

In terms of the global coordinates defined in the following

$$\underline{w} = \begin{Bmatrix} \underline{w} \\ \phi \end{Bmatrix}, \quad \bar{\underline{w}}^* = \begin{Bmatrix} \underline{w}^* \\ \phi \end{Bmatrix} \quad (39)$$

and

$$\begin{aligned}
 \underline{w}^T &= \{w_1^{(1)} \quad w_2^{(1)} \quad w_3^{(1)} \quad w_4^{(1)} \quad w_3^{(2)} \quad w_4^{(2)} \dots w_3^{(L)} \quad w_4^{(L)}\} \\
 \underline{w}^{*T} &= \{w_1^{*(1)} \quad w_2^{*(1)} \quad w_3^{*(1)} \quad w_4^{*(1)} \quad w_3^{*(2)} \quad w_4^{*(2)} \dots w_3^{*(L)} \quad w_4^{*(L)}\} \quad (40)
 \end{aligned}$$



One has from Eq. (37):

$$\begin{aligned}
 (\delta I)_{w, \phi} &= 0 \\
 &= \delta \bar{W}^{*T} (\bar{K} + \lambda^2 \bar{M}) \bar{W} \\
 &= \{\delta \bar{W}^{*T} \delta \phi^*\} \begin{bmatrix} \bar{K}_{11} + \lambda^2 \bar{M}_{11} & \bar{K}_{12} + \lambda^2 \bar{M}_{12} \\ \bar{K}_{21} + \lambda^2 \bar{M}_{21} & \bar{K}_{22} + \lambda^2 \bar{M}_{22} \end{bmatrix} \begin{Bmatrix} \bar{W} \\ \phi \end{Bmatrix} \quad (41)
 \end{aligned}$$

The global matrices  $\bar{K}_{ij}$ ,  $\bar{M}_{ij}$ ,  $i, j = 1, 2$  are assembled from the element matrices defined in Eqs. (38) in the following manner.

$$\begin{aligned}
 \delta \bar{W}^{*T} \bar{K}_{11} \bar{W} &= \sum_{i=1}^L \delta \bar{W}^{*(i)T} \{L^3 (C + bB) + bL(2D - B - E) \\
 &+ 2ibL(B - D) - i^2 bLB\} \bar{W}^{(i)} + \delta \bar{W}^{*(1)T} \{k_1 F + k_2 L^2 G\} \bar{W}^{(1)} \quad (42a)
 \end{aligned}$$

$$\delta \bar{W}^{*T} \bar{K}_{12} \phi = \sum_{i=1}^L \delta \bar{W}^{*(i)T} (-2ebL p) \phi \quad (42b)$$

$$\delta \phi^* \bar{K}_{21} \bar{W} = \delta \phi^* \sum_{i=1}^L 2(e - e_A) bL [s^T - r^T + ir^T] \bar{W}^{(i)} \quad (42c)$$

$$\delta \phi^* \bar{K}_{22} \phi = \delta \phi^* (\Omega^2 k^2 + k_3) \phi \quad (42d)$$

$$\delta \bar{W}^{*T} \bar{M}_{11} \bar{W} = \sum_{i=1}^L \delta \bar{W}^{*(i)T} \frac{1}{L} A \bar{W}^{(i)} \quad (42e)$$

$$\delta \bar{W}^{*T} \bar{M}_{12} \phi = \sum_{i=1}^L \delta \bar{W}^{*(i)T} \frac{e}{L} p \phi \quad (42f)$$

$$\delta \phi^* \bar{M}_{21} \bar{W} = \delta \phi^* \sum_{i=1}^L \frac{e}{L} p^T \bar{W}^{(i)} \quad (42g)$$

$$\delta \phi^* \bar{M}_{22} \phi = \delta \phi^* k_m^2 \phi \quad (42h)$$

Since  $\delta \tilde{w}^{*T} = \{\delta \tilde{w}^{*T} \delta \phi^*\}$  in Eq. (41) is unconstrained, Eq. (41) leads directly to

$$(\bar{K} + \lambda^2 \bar{M}) \bar{w} = 0 \quad (43)$$

which is the final matrix eigenvalue equation to be solved.

5. RESULTS AND DISCUSSION. Prior to the presentation of the demonstrative numerical results, it will be worthwhile to make some observations on the nondimensionalized differential equations (15) and (16) and the boundary conditions (24).

a. For  $e = 0$ , the flapping motion  $w(x,t)$  and the root torsion  $\phi(t)$  are essentially uncoupled. The eigenvalue solutions of  $w$  reduce to that of a rotating beam and agree well with the available data of Boyce, DiPrima and Handelman [11]. The torsional vibration frequency has only one eigenvalue solution and, if  $e_A = 0$  also, it varies linearly with the rotor speed  $\Omega$  as expected.

b. For  $e \neq 0$  and  $e_A = 0$ , the motions are generally coupled. It is observed that if  $e$  and  $\phi$  both change sign, the equation remains unaltered. Thus, as far as eigenvalues are concerned, they depend only on the absolute values of  $e$ . The solution of  $\phi$  for a negative  $e$ , however, is  $180^\circ$  out of phase compared with the one for a positive  $e$  of the same magnitude.

c. For  $e \neq 0$  and  $e_A \neq 0$  the motions are generally coupled. It is observed that if  $e$ ,  $e_A$  and  $\phi$  all three change signs, the governing equations remain unaltered.

Some demonstrative calculations will now be given\*. The eigenvalue  $\lambda$  is generally a complex number.

$$\lambda = \lambda_R + i\lambda_I \quad (44)$$

From equations (17) and (44), it is clear that the system is unstable of divergence when  $\lambda_R$  is nonzero positive and  $\lambda_I = 0$ . When  $\lambda_R = 0$ , on the other hand,  $\lambda_I$  (LAMBDA)\*\* represents the nondimensional frequency of vibration and it can then be plotted against the nondimensional blade rotating speed  $\Omega$  (OMEGA), as shown in Figures 3 through 7. When  $\lambda$  is complex, one of the square roots of  $\lambda^2$  must have nonzero positive real part. The system is then unstable since  $\lambda$  appears in the equations only as  $\lambda^2$ . The value of  $\lambda$  generally become complex as the two branches of the frequency curve coalesce. The "critical" speeds can be located in these figures by noting these points of coalescence.

\*An extensive parametric study of a rotor blade instability in vacuum due to the coupled flap-(root)torsion motion will be presented in a forthcoming paper.

\*\*The symbols enclosed in parentheses are those used in Figures 3 through 7.



For the following sample calculations, the parameters used are typical for a medium size rotor blade of 20 ft. in length, for example. It is further assumed that (the nondimensionalized quantities)

$$e(E) = 0.003, \quad e_o(E_o) = 0$$

$$k_{m1}(KM1) = 0.0025, \quad k_{m2}(KM2) = 0.0100$$

The boundary conditions at the hub are those of a hingeless blade. The values of  $k_1(K-1)$  and  $k_2(K-2)$  are set to  $10^8$  as approximations to infinity. The torsional spring constant  $k_3(K-3)$  has been set to zero.

In Figure 3,  $e_A(E_A)$  is taken to be 0.003. Thus

$$\gamma (\text{GAMMA}) = \frac{e_A}{e} = \frac{-e_A}{-e} = 1.00 .$$

Here the lowest branch of  $\lambda_I$  is essentially for the torsional motion. The second and third lowest branches are essentially the first and the second for flapping motion. For the range of rotor speed shown\*,  $0 \leq \Omega < 25$ , the coupling is not sufficient to have instability. In the subsequent figures as  $e_A = 0.0015, 0, -0.0015$  and  $-0.003$  (and  $\gamma = 0.5, 0, -0.5$  and  $-1.0$ ), the effect of coupling becomes more and more severe. In Figure 4, the two lowest branches of eigenvalues appear to draw closer compared with those in Figure 3. They actually coalesce in Figure 5 at a critical speed about  $\Omega = 16.5$ . As  $e_A$  continue to decrease (increase) in algebraic sense while holding  $e$  a positive (negative) constant the critical speed of flutter instability tends to decrease and thus the structure becomes more critical. This is observed in Figures 6 and 7.

To obtain some idea on the effect due to the torsional spring  $k_3$ , the calculations are repeated for the same set of data as in Figure 5 except that the value of  $k_3$  is changed from zero to 0.01. The new frequency curves are shown in Figure 8. It appears in this figure that the essentially torsional branch has moved upward while the other branches remain largely unaltered. The new critical speed prior to flutter instability, however, has changed from 16.46 (Figure 5) to 17.08.

A rather quick review of the existing literature suggests that the flutter instability due to the coupling flapping and root torsion motions may have not been reported previously. The practical significance of such instability within the range of real design parameters is obvious. An extensive parametric study on this instability is being carried out. The results will be reported shortly.

ACKNOWLEDGEMENT. The authors wish to express their appreciation to Mr. Richard F. Haggerty for his assistance in obtaining the numerical results. They also wish to thank Miss Ellen Fogarty for her patience and skill in typing the manuscript.

\*At  $\Omega$  (OMEGA) = 25, which is nondimensional, the real rotor speed is roughly 1000 rpm for a typical value of  $c = \sqrt{(\rho A \ell^4 / EI)} = 0.0040 \text{min.}$

#### REFERENCES

1. P. Friedman and P. Tong, "Nonlinear Equations for Bending of Rotating Beams with Application to Linear Flap-lag Stability of Hingeless Rotors," NASA CR-114485, May 1972.
2. D. H. Hodges and R. A. Ormiston, "Stability of Elastic Bending and Torsion of Uniform Cantilevered Rotor Blades in Hover," 14th Structures, Structural Dynamics and Materials Conference, AIAA Paper No. 73-405, 1973.
3. R. H. Miller and C. W. Ellis, "Helicopter Blade Vibration and Flutter," Journal of American Helicopter Society, Vol. 1, No. 3, pp. 19-38, 1956.
4. N. D. Ham, "Helicopter Blade Flutter," AGARD Report No. 607, 1973.
5. D. H. Hodges and R. A. Ormiston, "Nonlinear Equations for Bending of Rotating Beams with Application to Linear Flap-lag Stability of Hingeless Rotors," NASA TM X-2770, 1973.
6. J. J. Wu, "On Adjoint Operators Associated with Boundary Value Problems," Journal of Sound and Vibration, Vol. 39, No. 2, pp. 195-206, 1975.
7. J. J. Wu, "A Unified Finite Element Approach to Column Stability Problems," Developments in Mechanics, Vol. 8, pp. 279-294, 1975.
8. J. J. Wu, "Effects of Support Flexibility on the Stability of a Beam Under a Followed Thrust and Inertia," Developments in Theoretical and Applied Mechanics, Vol. 8, pp. 391-402, 1976.
9. J. J. Wu, "Column Instability Under Nonconservative Forces, With Internal and External Damping - Finite Element Using Adjoint Variational Principles," Developments in Mechanics, Vol. 7, pp. 501-514, 1973.
10. J. C. Houbolt and G. W. Brooks, "Differential Equations of Motion for Combined Flapwise Bending, Chordwise Bending and Torsion of Twisted Rotor Blades," NACA Report No. 1346, 1956.
11. W. E. Boyce, R. C. DiPrima and G. H. Handelman, "Vibrations of Rotating Beams of Constant Section," Proceedings of the Second U.S. National Congress of Applied Mechanics, Ann Arbor, Mich., pp. 165-173 (1954).



APPENDIX

The numerical value of some of the matrices used in Section 4 are given here.

$$\tilde{A} = \int_0^1 \tilde{a} \tilde{a}^T d\xi = \begin{bmatrix} \frac{13}{25} & \frac{11}{210} & \frac{9}{70} & -\frac{13}{420} \\ \frac{11}{210} & \frac{1}{105} & \frac{13}{420} & -\frac{1}{140} \\ \frac{9}{70} & \frac{13}{420} & \frac{13}{35} & -\frac{11}{210} \\ -\frac{13}{420} & -\frac{1}{140} & -\frac{11}{210} & \frac{1}{105} \end{bmatrix} \quad (\text{A-1})$$

$$\tilde{B} = \int_0^1 \tilde{a}' \tilde{a}'^T d\xi = \begin{bmatrix} \frac{6}{5} & \frac{1}{10} & -\frac{6}{5} & \frac{1}{10} \\ \frac{1}{10} & \frac{2}{15} & -\frac{1}{10} & -\frac{1}{30} \\ -\frac{6}{5} & -\frac{1}{10} & \frac{6}{5} & -\frac{1}{10} \\ \frac{1}{10} & -\frac{1}{30} & -\frac{1}{10} & \frac{2}{15} \end{bmatrix} \quad (\text{A-2})$$

$$\tilde{C} = \int_0^1 \tilde{a}'' \tilde{a}''^T d\xi = \begin{bmatrix} 12 & 6 & -12 & 6 \\ 6 & 4 & -6 & 2 \\ -12 & -6 & 12 & -6 \\ 6 & 2 & -6 & 4 \end{bmatrix} \quad (\text{A-3})$$

$$\underline{D} = \int_0^1 \xi \underline{a}' \underline{a}'^T d\xi = \begin{bmatrix} \frac{3}{5} & \frac{1}{10} & -\frac{3}{5} & 0 \\ \frac{1}{10} & \frac{1}{30} & \frac{1}{10} & \frac{1}{60} \\ -\frac{3}{5} & -\frac{1}{10} & \frac{3}{5} & 0 \\ 0 & -\frac{1}{60} & 0 & \frac{1}{10} \end{bmatrix} \quad (\text{A-4})$$

$$\underline{E} = \int_0^1 \xi^2 \underline{a}' \underline{a}'^T d\xi = \begin{bmatrix} \frac{12}{35} & \frac{1}{14} & -\frac{12}{35} & -\frac{1}{35} \\ \frac{1}{14} & \frac{1}{105} & -\frac{1}{14} & -\frac{1}{70} \\ -\frac{12}{35} & -\frac{1}{14} & \frac{12}{35} & \frac{1}{35} \\ -\frac{1}{35} & -\frac{1}{70} & \frac{1}{35} & \frac{3}{35} \end{bmatrix} \quad (\text{A-5})$$

$$\underline{F} = \underline{a}(0) \underline{a}'^T(0) = \begin{bmatrix} 1 & 0 & 0 & 0 \\ 0 & 0 & 0 & 0 \\ 0 & 0 & 0 & 0 \\ 0 & 0 & 0 & 0 \end{bmatrix} \quad (\text{A-6})$$

$$\underline{G} = \underline{a}'(0) \underline{a}'^T(0) = \begin{bmatrix} 0 & 0 & 0 & 0 \\ 0 & 1 & 0 & 0 \\ 0 & 0 & 0 & 0 \\ 0 & 0 & 0 & 0 \end{bmatrix} \quad (\text{A-7})$$



$$\underline{p} = \int_0^1 \underline{a} d\xi = \begin{bmatrix} \frac{1}{2} \\ \frac{1}{12} \\ \frac{1}{2} \\ -\frac{1}{12} \end{bmatrix} \quad (\text{A-8})$$

$$\underline{r} = \int_0^1 \underline{a}' d\xi = \begin{bmatrix} -1 \\ 0 \\ 1 \\ 0 \end{bmatrix} \quad (\text{A-9})$$

$$\underline{s} = \int_0^1 \xi \underline{a}' d\xi = \begin{bmatrix} \frac{1}{2} \\ -\frac{1}{12} \\ \frac{1}{2} \\ \frac{1}{12} \end{bmatrix} \quad (\text{A-10})$$

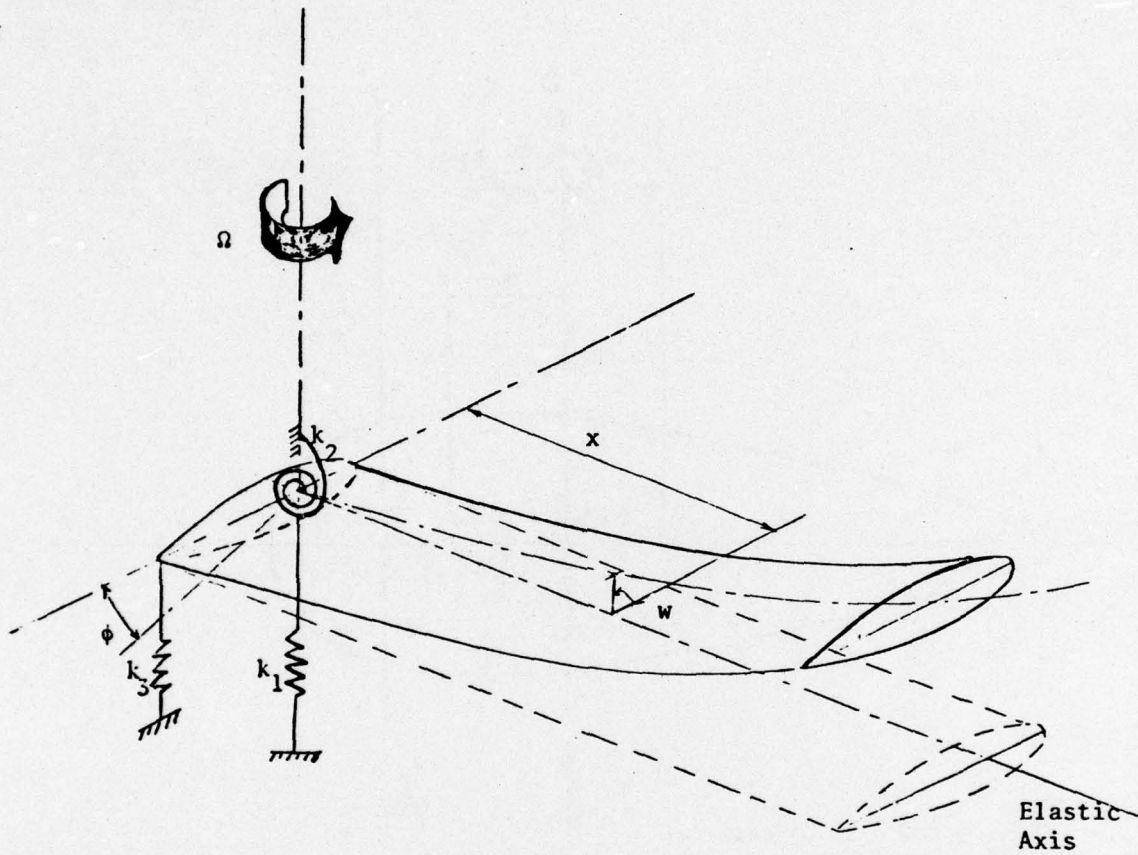
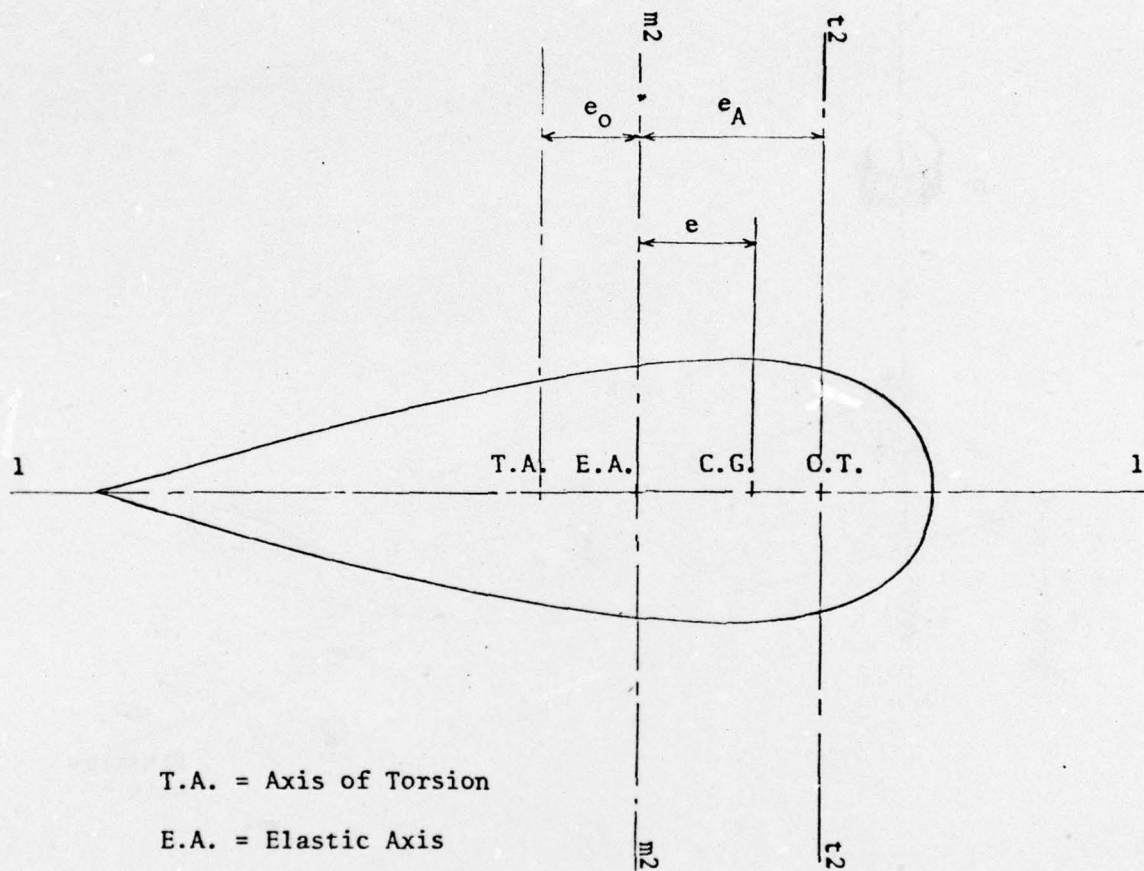


Figure 1. Problem configuration. (Elastic axis is shown to coincide with the axis of torsion in the figure.)





T.A. = Axis of Torsion

E.A. = Elastic Axis

C.G. = Centre of Gravity

C.T. = Centroid of Tensile Area of a Cross Section

Figure 2. Parameters related to off-sets of various axes.

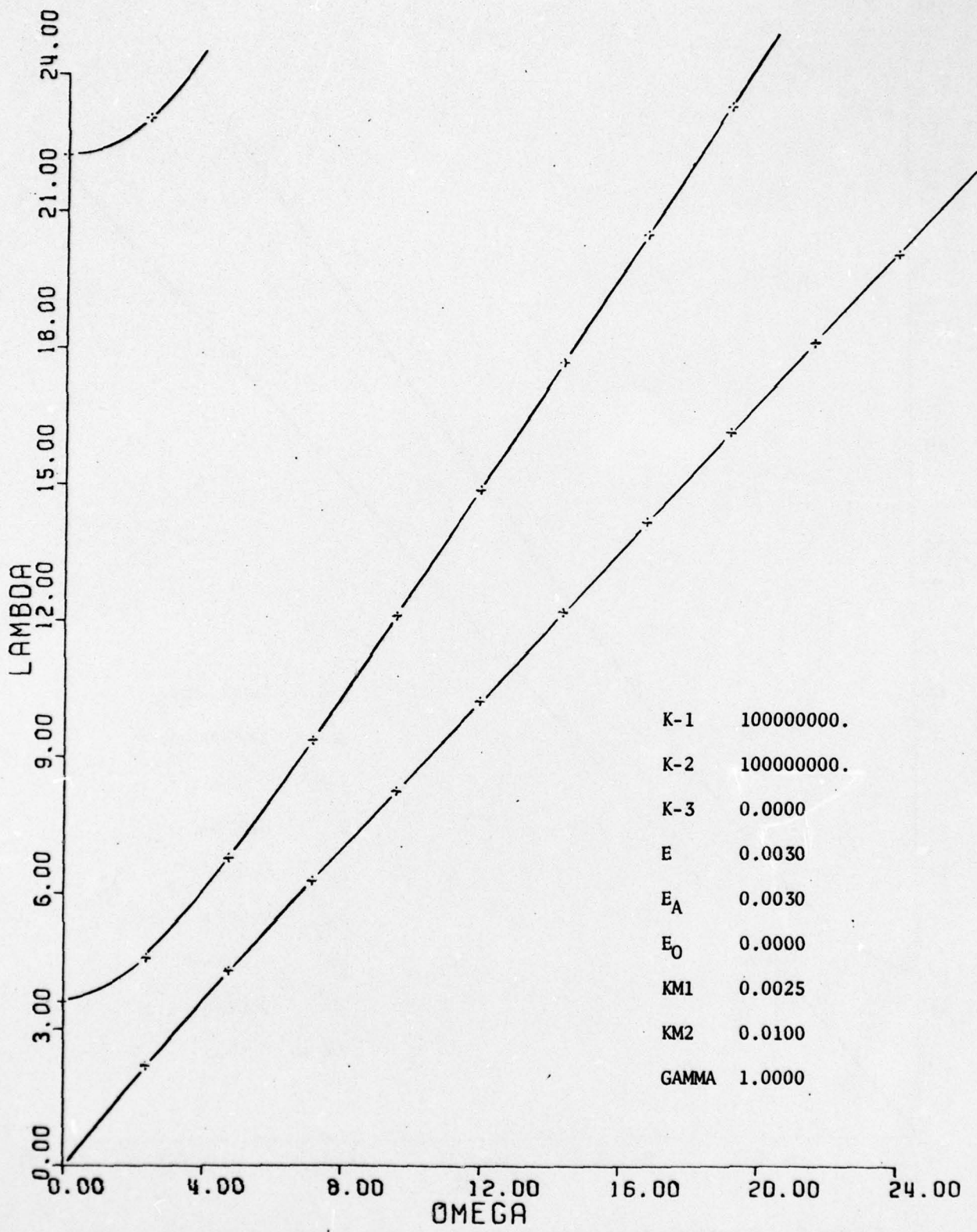


Figure 3. Vibration frequency vs speed of rotation ( $e_A=0.0030$ ,  $e=0.0030$ ).  
 No instability in the range of speed shown.



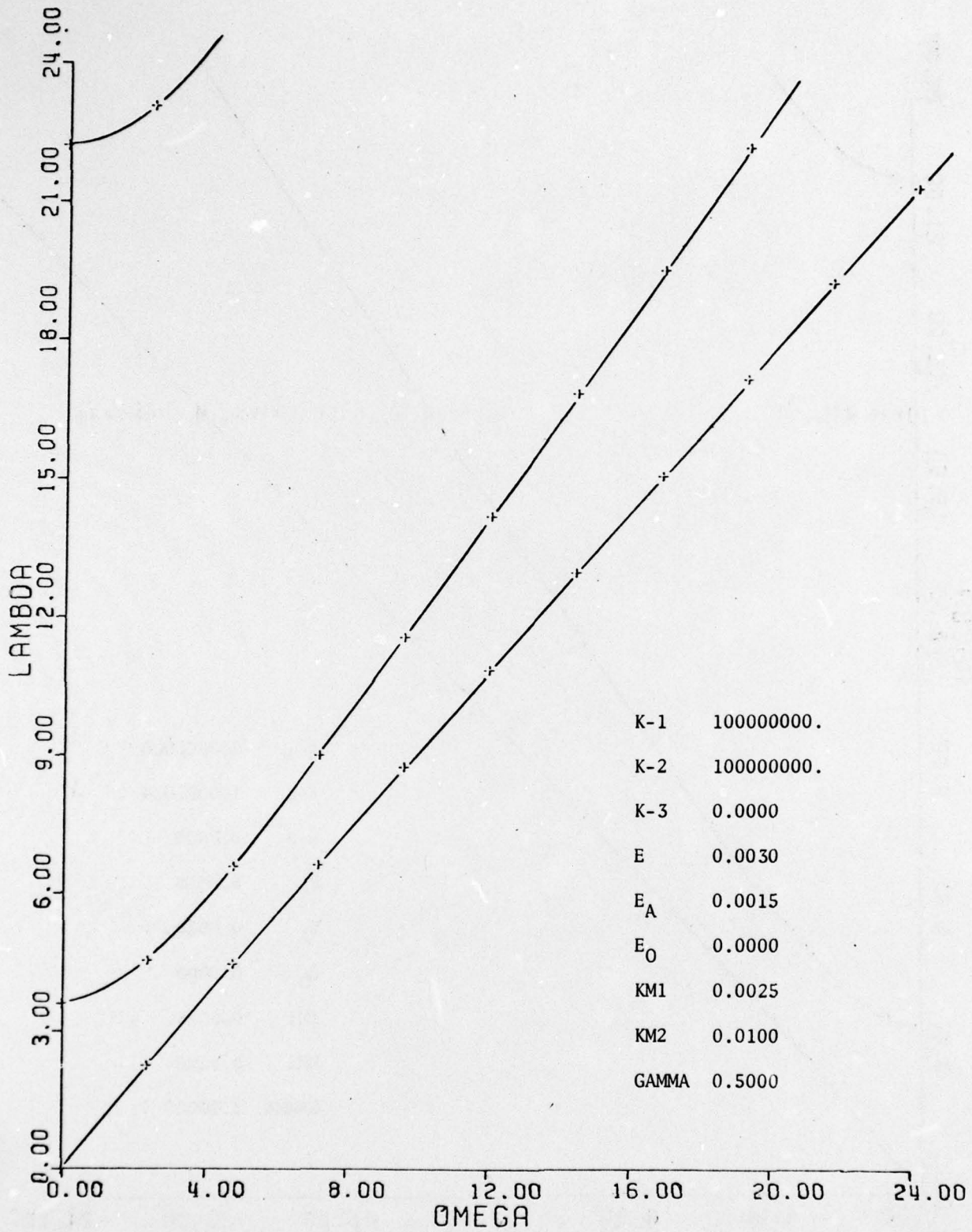


Figure 4. Vibration frequency vs speed of rotation ( $e_A=0.0015$ ,  $e=0.0030$ ).  
No instability in the range of speed shown.

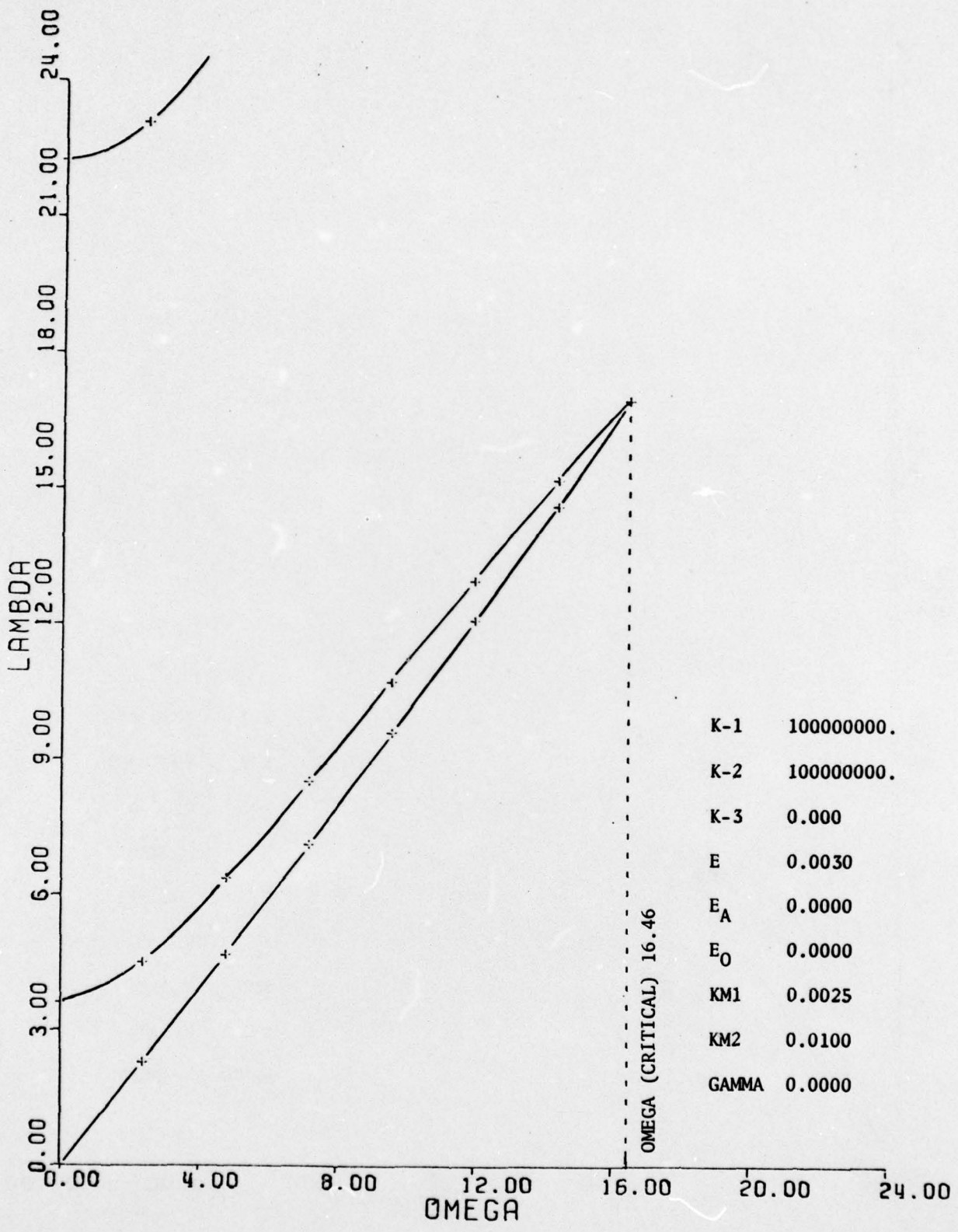


Figure 5. Vibration frequency vs speed of rotation ( $e_A=0$ ,  $e=0.0030$ ).  
Flutter instability at  $\Omega=16.46$ .



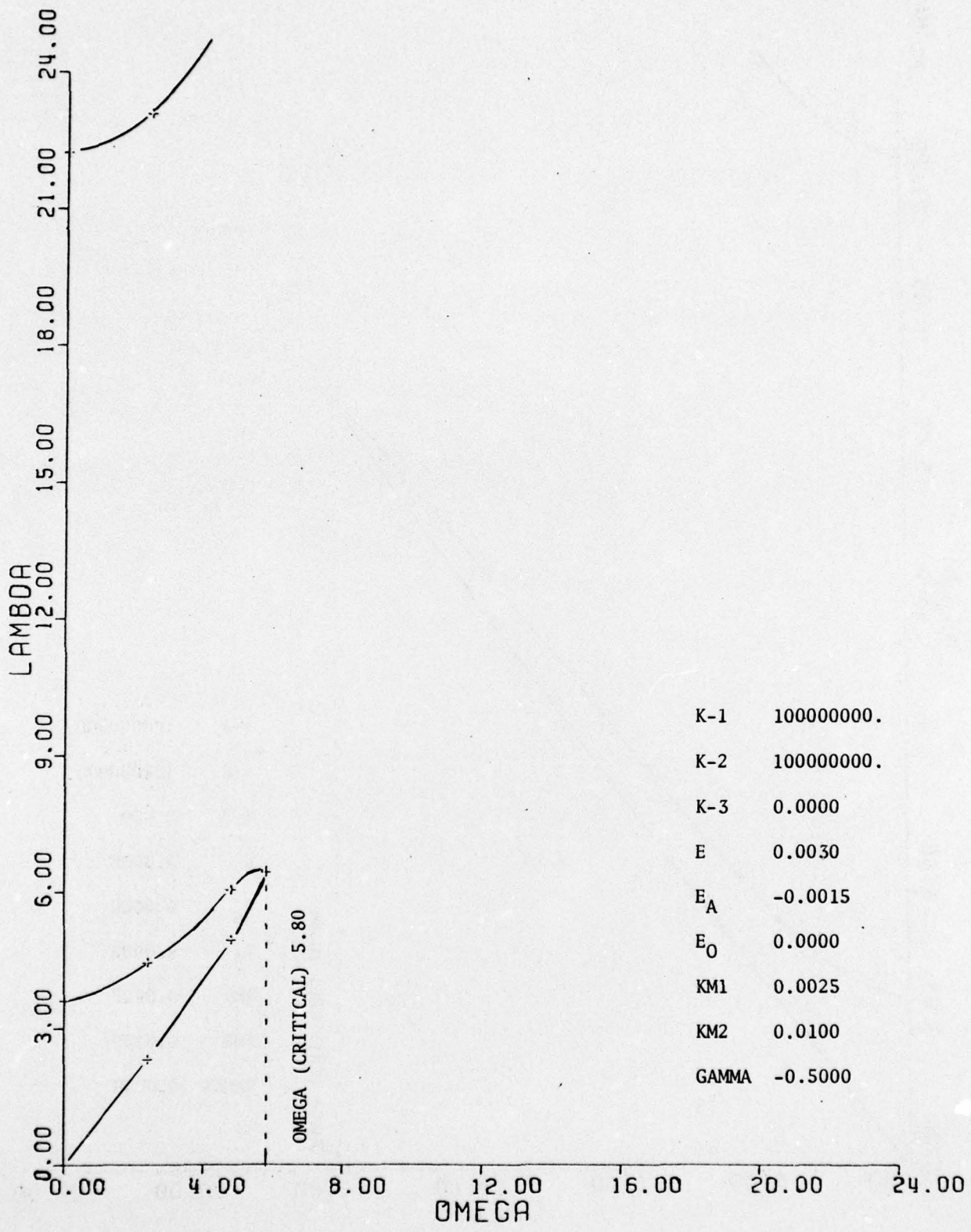


Figure 6. Vibration frequency vs speed of rotation ( $e_A = -0.0015$ ,  $e = 0.0030$ ). Flutter instability at  $\Omega = 5.80$ .

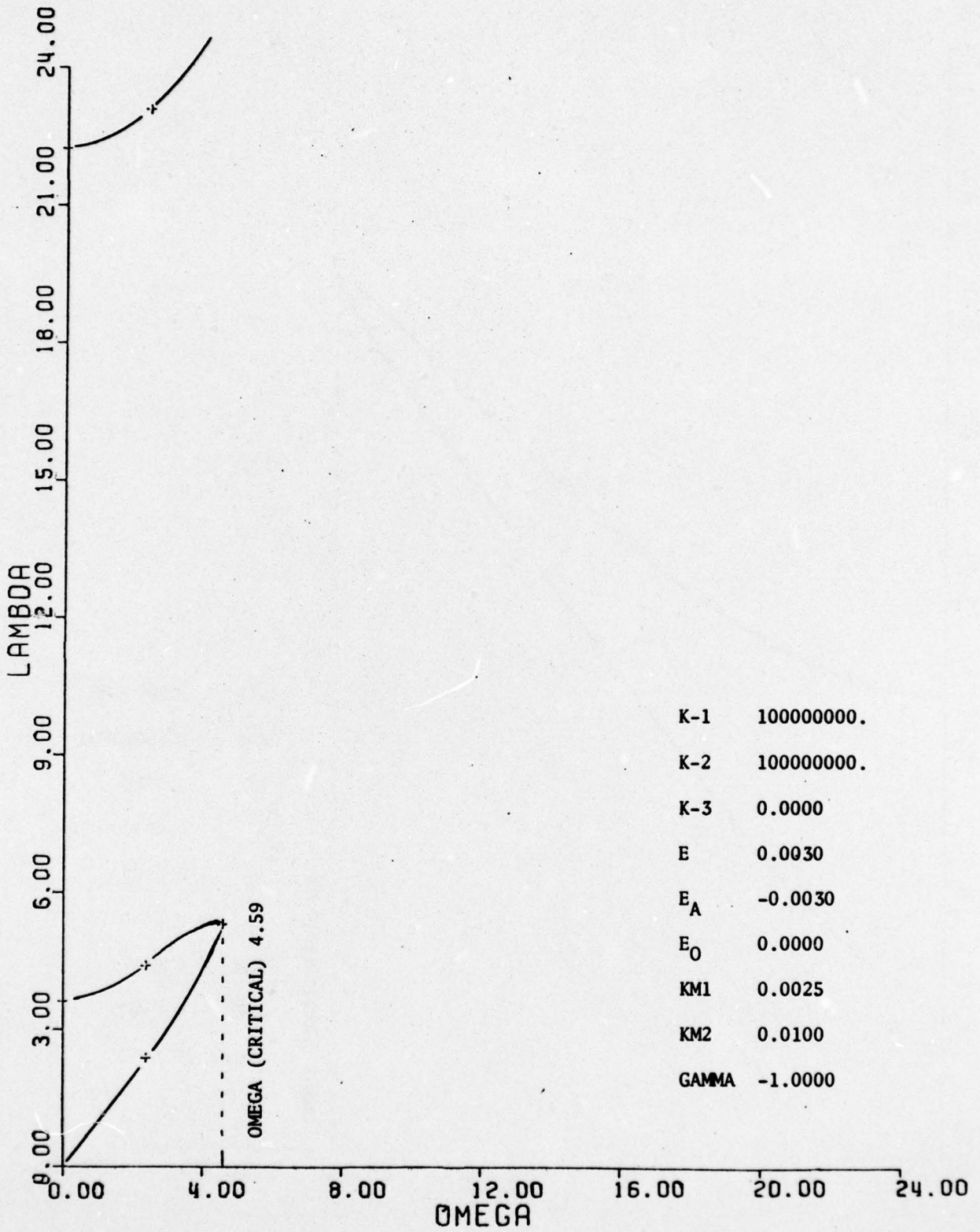


Figure 7. Vibration frequency vs speed of rotation ( $e_A = -0.0030$ ,  $e = 0.0030$ ). Flutter instability at  $\Omega = 4.59$ .



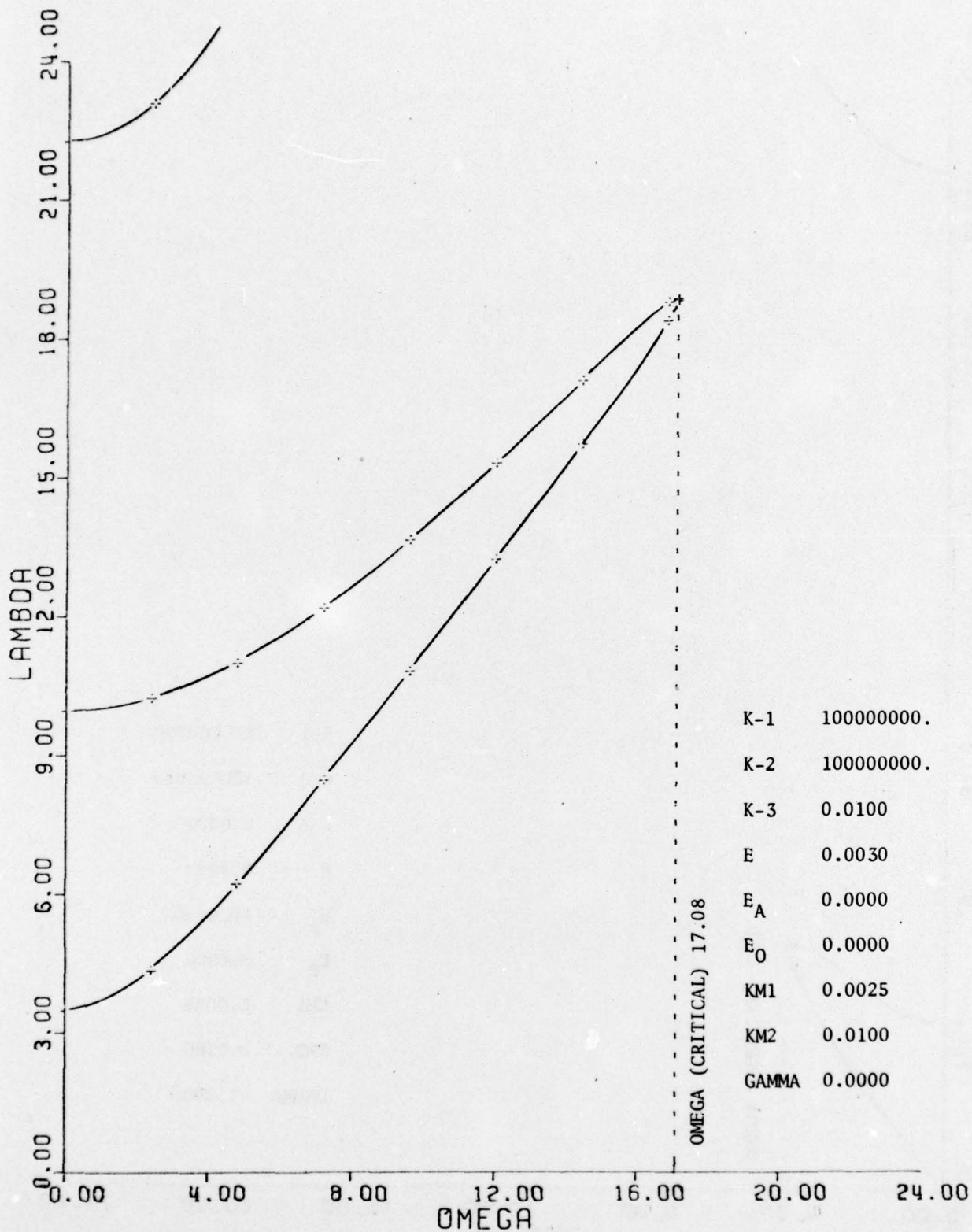


Figure 8. Vibration frequency vs speed of rotation. (Same data as in Figure 5, except  $k_3$  has been changed from zero to 0.01). Flutter instability at  $\Omega=17.08$ .

WATERVLiet ARSENAL INTERNAL DISTRIBUTION LIST

May 1976

	<u>No. of Copies</u>
COMMANDER	1
DIRECTOR, BENET WEAPONS LABORATORY	1
DIRECTOR, DEVELOPMENT ENGINEERING DIRECTORATE	1
ATTN: RD-AT	1
RD-MR	1
RD-PE	1
RD-RM	1
RD-SE	1
RD-SP	1
DIRECTOR, ENGINEERING SUPPORT DIRECTORATE	1
DIRECTOR, RESEARCH DIRECTORATE	2
ATTN: RR-AM	1
RR-C	1
RR-ME	1
RR-PS	1
TECHNICAL LIBRARY	5
TECHNICAL PUBLICATIONS & EDITING BRANCH	2
DIRECTOR, OPERATIONS DIRECTORATE	1
DIRECTOR, PROCUREMENT DIRECTORATE	1
DIRECTOR, PRODUCT ASSURANCE DIRECTORATE	1
PATENT ADVISORS	1



EXTERNAL DISTRIBUTION LIST

December 1976

1 copy to each

OFC OF THE DIR. OF DEFENSE R&E  
ATTN: ASST DIRECTOR MATERIALS  
THE PENTAGON  
WASHINGTON, D.C. 20315

CDR  
US ARMY TANK-AUTMV COMD  
ATTN: AMDTA-UL  
AMSTA-RKM MAT LAB  
WARREN, MICHIGAN 48090

CDR  
PICATINNY ARSENAL  
ATTN: SARPA-TS-S  
SARPA-VP3 (PLASTICS  
TECH EVAL GEN)  
DOVER, NJ 07801

CDR  
FRANKFORD ARSENAL  
ATTN: SARFA  
PHILADELPHIA, PA 19137

DIRECTOR  
US ARMY BALLISTIC RSCH LABS  
ATTN: AMXBR-LB  
ABERDEEN PROVING GROUND  
MARYLAND 21005

CDR  
US ARMY RSCH OFC (DURHAM)  
BOX CM, DUKE STATION  
ATTN: RDRD-IPL  
DURHAM, NC 27706

CDR  
WEST POINT MIL ACADEMY  
ATTN: CHMN, MECH ENGR DEPT  
WEST POINT, NY 10996

CDR  
HQ, US ARMY AVN SCH  
ATTN: OFC OF THE LIBRARIAN  
FT RUCKER, ALABAMA 36362

CDR  
US ARMY ARMT COMD  
ATTN: AMSAR-PPW-IR  
AMSAR-RD  
AMSAR-RDG  
ROCK ISLAND, IL 61201

CDR  
US ARMY ARMT COMD  
FLD SVC DIV  
ARMCOM ARMT SYS OFC  
ATTN: AMSAR-ASF  
ROCK ISLAND, IL 61201

CDR  
US ARMY ELCT COMD  
FT MONMOUTH, NJ 07703

CDR  
REDSTONE ARSENAL  
ATTN: AMSMI-RRS  
AMSMI-RSM  
ALABAMA 35809

CDR  
ROCK ISLAND ARSENAL  
ATTN: SARRI-RDD  
ROCK ISLAND, IL 61202

CDR  
US ARMY FGN SCIENCE & TECH CEN  
ATTN: AMXST-SD  
220 7TH STREET N.E.  
CHARLOTTESVILLE, VA 22901

DIRECTOR  
US ARMY PDN EQ. AGENCY  
ATTN: AMXPE-MT  
ROCK ISLAND, IL 61201

EXTERNAL DISTRIBUTION LIST (Cont)

1 copy to each

CDR  
US NAVAL WPNS LAB  
CHIEF, MAT SCIENCE DIV  
ATTN: MR. D. MALYEVAC  
DAHLGREN, VA 22448

DIRECTOR  
NAVAL RSCH LAB  
ATTN: DIR. MECH DIV  
WASHINGTON, D.C. 20375

DIRECTOR  
NAVAL RSCH LAB  
CODE 26-27 (DOCU LIB.)  
WASHINGTON, D.C. 20375

NASA SCIENTIFIC & TECH INFO FAC  
PO BOX 8757, ATTN: ACQ BR  
BALTIMORE/WASHINGTON INTL AIRPORT  
MARYLAND 21240

DEFENSE METALS INFO CEN  
BATTELLE INSTITUTE  
505 KING AVE  
COLUMBUS, OHIO 43201

MANUEL E. PRADO / G. STISSER  
LAWRENCE LIVERMORE LAB  
PO BOX 808  
LIVERMORE, CA 94550

DR. ROBERT QUATTRONE  
CHIEF, MAT BR  
US ARMY R&S GROUP, EUR  
BOX 65, FPO N.Y. 09510

2 copies to each

CDR  
US ARMY MOB EQUIP RSCH & DEV COMD  
ATTN: TECH DOCU CEN  
FT BELVOIR, VA 22060

CDR  
US ARMY MAT RSCH AGCY  
ATTN: AMXMR - TECH INFO CEN  
WATERTOWN, MASS 02172

CDR  
WRIGHT-PATTERSON AFB  
ATTN: AFML/MXA  
OHIO 45433

CDR  
REDSTONE ARSENAL  
ATTN: DOCU & TECH INFO BR  
ALABAMA 35809

12 copies

CDR  
DEFENSE DOCU CEN  
ATTN: DDC-TCA  
CAMERON STATION  
ALEXANDRIA, VA 22314

NOTE: PLEASE NOTIFY CDR, WATERVLIET ARSENAL, ATTN: SARWV-RT-TP,  
WATERVLIET, N.Y. 12189, IF ANY CHANGE IS REQUIRED TO THE ABOVE.